Site-Specific Glycoprofiles of HDL-Associated ApoE are Correlated with HDL Functional Capacity and Unaffected by Short-Term Diet

Chenghao Zhu,[†] Maurice Wong,[‡] Qiongyu Li,[‡] Lisa Sawrey-Kubicek,[†] Elizabeth Beals,[†] Chris H. Rhodes,[†] Romina Sacchi,[†] Carlito B. Lebrilla,[‡] and Angela M. Zivkovic*,[†]

[†]Department of Nutrition and [‡]Department of Chemistry, University of California, Davis, Davis, California 95616, United States

S *Supporting Information*

ABSTRACT: Since high-density lipoprotein (HDL) glyco-profiles are associated with HDL functional capacity, we set out to determine whether diet can alter the glycoprofiles of key HDL-associated proteins, including ApoE, a potent driver of chronic disease risk. Ten healthy subjects consumed a fast food (FF) and a Mediterranean (Med) diet for 4 days in randomized order, with a 4-day wash-out between treatments. A multiple reaction monitoring method was used to characterize the site-specific glycoprofiles of HDL proteins, and HDL functional capacity was analyzed. We describe for the first time that ApoE has 7 mucin-type O-glycosylation sites, which were not affected by short-term diet. The glycoprofiles of other HDL-associated proteins were also unaffected, except that a disialylated ApoC-III glycan was enriched after Med diet, and a nonsialylated ApoC-III glycan was enriched after FF diet. Twenty-five individual glycopeptides were significantly correlated with cholesterol efflux capacity and 21 glycopeptides were correlated with immunomodulatory capacity. Results from this study indicate that the glycoprofiles of HDL-associated proteins including ApoE are correlated with HDL functional capacity but generally unaffected by diet in the short term, except ApoC-III sialylation. These results suggest that HDL protein glycoprofiles are affected by both acute and long-term factors and may be useful for biomarker discovery.

KEYWORDS: *cholesterol efflux, high-density lipoprotein, glycomics, glycoproteomics, ApoE, ApoC-III, fast food diet, Mediterranean diet*
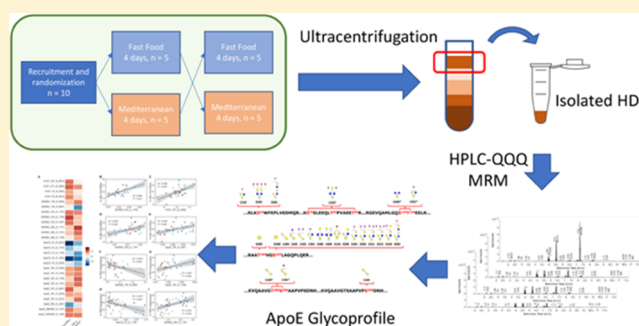
INTRODUCTION

High-density lipoprotein (HDL) particles are protein−lipid complexes that transport lipophilic molecules in the blood. Primarily known for their function in regulating cellular cholesterol concentrations through efflux of cholesterol out of cells and transport of cholesterol to the liver, HDL particles also perform a number of additional functions including immuno-modulatory, anti-inflammatory, anti-proteolytic, and other functions.[1−3] HDL particles are heterogeneous and undergo significant remodeling in vivo.[4] As many as 16 distinct HDL subclasses have been described, and based on their protein composition likely play distinct biological roles.[5] The proteomic composition of HDL particles is well-known to affect HDL function and is altered in a variety of disease states.[6−8] Recently, it has also been demonstrated that HDL-associated proteins are highly glycosylated.[9] HDL-associated proteins enriched in HDL particles have a different site-specific glycosylation pattern from the same proteins found in plasma,[10] and their glycosylation may be useful for diagnostic purposes.[11] Importantly, key HDL proteins are differentially glycosylated in multiple disease states vs healthy individuals, and site-specific glycosylation of HDL-associated proteins is associated with HDL's immunomodula-tory capacity.[12]

Apolipoprotein E (ApoE) genotype is one of the most important risk factors for a number of age-associated diseases,[13] and the single greatest genetic risk factor for Alzheimer's disease.[14] ApoE is a component of HDL particles that is involved in mediating HDL functional capacity.[15,16] Although ApoE is known to be a glycosylated protein, ApoE glycosylation has only been partially characterized. To date, no comprehensive site-specific glycosylation analysis across all detectable glycosylation sites has been obtained for ApoE.

Dietary changes can modify HDL cholesterol efflux capacity,[17] and anti-inflammatory capacity (reviewed in ref 18); however, it is not clear whether diet alters HDL glycoprofiles or whether HDL glycoprofiles are also associated with HDL's cholesterol efflux capacity. The half-life of ApoA-I, the main protein constituent of HDL, is approximately 4 days;[19] we previously showed that the HDL lipidome is drastically remodeled by diet in 4 days.[20] Hence, we postulated that if there is an effect of diet on HDL glycoprofiles, it may be visible within this time frame.

In this pilot study, we hypothesized that a 4 day dietary intervention period measurably alters HDL site-specific

glycoprofiles and HDL functionality. Specifically, the effects of consuming a fast food (FF) diet vs a Mediterranean (Med) diet were compared to broadly test the hypothesis that large-scale shifts in the overall dietary pattern in the short term can alter HDL glycoprofiles and functionality. The FF arm of the study was designed to reflect a typical Western diet, which is enriched in red meat, simple sugars, fat, saturated fat, and cholesterol, and low in fresh fruits, vegetables, and fiber.[21−25] The Med arm of the study was designed to reflect what is currently widely thought to be a healthy diet enriched in fresh fruits, vegetables, fiber, monounsaturated fat, and polyunsaturated fat, particularly omega-3 fatty acids.[26−31] HDL function and site-specific glycoprofiles in response to the two dietary patterns were assessed and compared.

■ MATERIALS AND METHODS

Study Design and Subjects

Ten healthy human subjects (5 male and 5 female) were recruited into a randomized order, cross-over study. Each subject was given both the FF and Med diet for 4 days in duration in randomized order with a 4-day washout between treatments. The study dietary plan was balanced for each participant's daily caloric requirements calculated using the Harris−Benedict equation. The study foods for the Med diet were purchased at a local grocery store and prepared for participants to consume at home, while the foods for the FF diet were purchased from a local fast food restaurant. An overnight fasted blood draw was taken from the antecubital vein by a licensed phlebotomist, and anthropometric measurements were taken on the first and the morning after the last day of each study arm. Plasma or serum was separated within 1 h of the blood draw. The samples were aliquoted immediately and stored at −80 °C. One sample was sent for a lipid panel test to the University of California Davis Medical Center pathology laboratory.

Study subjects were 18−25 years old, nonsmokers, with BMI ranging from 21.2 to 32.9 kg/m^2. Subjects were free from any disease diagnoses including anemia, diabetes, thyroid disease, metabolic syndrome, cancer, and cardiovascular diseases. Subjects with extreme dietary or exercise patterns, or taking medications or supplements that alter lipoproteins were excluded from the study. The study was approved by the University of California Davis Institutional Review board and registered at clinicaltrials.gov (NCT03205254).

Diet

On the FF arm, depending on the participant's calculated caloric requirement, 1 or 2 frosted strawberry pop-tarts were given for breakfast, and different hamburgers with or without fries were assigned to subjects for lunch and dinner, with soda consumed ad libitum. On the Med arm, breakfast included high-fiber cereal in 1% milk with one small banana. Lunch was a study salad with canned tuna or chicken, while dinner was minestrone soup, multigrain blend, tomato basil marinara, mixed vegetables, and extra virgin olive oil (EVOO) adjusted to the calorie level. Almonds and other dried fruits and nuts were provided as snacks between meals according to the prescribed calorie level. The snacks on the Med diet were provided to meet each individual's daily calorie requirement and to maintain the FF and Med arms isocaloric. The study diet menu for FF and Med at the 2000 kcal/day level is shown in Supplementary Table S1.

HDL Isolation

A 2-step density-based sequential flotation ultracentrifugation method was used to isolate HDL particles as previously described.[12] Two milliliters of plasma was adjusted using a concentrated potassium bromide (KBr) solution (density 1.340 g/mL) to a density of 1.063 g/mL, before being underlaid to KBr solution of 1.063 g/mL into an ultracentrifugation tube (OptiSeal, Beckman Coulter). A 2 mL supernatant was removed after an ultracentrifugation spin at 110 000 rpm for 3 h and 10 min. The HDL-containing bottom layer was then adjusted to a density of 1.21 g/mL by adding the same concentrated KBr solution, followed by underlaying to the KBr solution of 1.21 g/ mL in two ultracentrifugation tubes. After the second ultra-centrifugation spin at 110 000 rpm for 3 h and 20 min, 1 mL supernatant of HDL fraction from each ultracentrifugation tube was combined and dialyzed twice using Amicon Ultra-4, MWCO 10 kDa filter units. The HDL fraction was reconstituted in either LC-MS water for glycoproteomics and ELISA assays, or PBS for functional assays. The samples were stored in −80 °C until analysis. All KBr solutions were freshly prepared and verified using a densitometer (Mettler Toledo, Columbus, OH). Ultracentrifugation was performed on a Beckman Optima MAX-TL equipped with a TLA-110 fixed-angle rotor (Beckman Coulter, k factor 13.04).

Apolipoprotein E Glycoprofile

The ApoE glycoprofile was identified using purified ApoE standard from human plasma obtained from Sigma-Aldrich (St. Louis, Missouri). The proteins were digested and analyzed as previously described.[10] In brief, proteins were denatured with dithiothreitol and alkylated with iodoacetamide. The denatured proteins were then digested with 2 μg of sequencing grade trypsin (Promega, Madison, WI) for 18 h at 37 °C. The protein tryptic digest was analyzed on a nanoLC Q-Exactive Orbitrap MS platform (Thermo Scientific, Waltham, MA) equipped with a 75 μm × 150 mm Magic C18 reversed phase column. Peptides and glycopeptides were identified using Byonic software (Protein Metrics, Inc.) set to a precursor and fragment mass tolerance of 10 ppm and a false discovery rate of <1%. Only peptides and glycopeptides with a log probability greater than 2 were considered.

HDL Glycoproteomics

The following glycoproteins were monitored and both the glycoprotein and the site-specific glycosylation quantities were determined for ApoE, apolipoprotein C-III (ApoC-III), α-1-antitrypsin (A1AT), and α-2-HS-glycoprotein (A2HSG, or fetuin A). Serum amyloid A (SAA) 1 and 2, which are the inducible and proinflammatory isoforms, are not glycosylated, thus only the protein quantity was measured. The mixture of peptides and glycopeptides was analyzed using an Agilent 1290 infinity LC system coupled with an Agilent 6490 triple quadrupole (QQQ) mass spectrometer (Agilent Technology, Santa Clara, CA) using a previously published method.[10] Briefly, isolated HDL samples and protein standards were digested using trypsin and then separated on the Agilent eclipse plus C18 (RRHD 1.8 μm, 2.1 mm × 100 mm) UHPLC analytical column. Analytes were monitored using a dynamic multiple reaction monitoring (dMRM) mode. Each glycopeptide transition was composed of the glycopeptide molecular ion of a certain charge as a precursor and the glycopeptide diagnostic oxonium ions such as m/z 204.08 (HexNAc), 366.14 (Hex1HexNAc1), 292.09 (Neu5Ac), and 274.09 (Neu5Ac − H$_2$O) as product ions. The MRM transitions monitored for ApoC-III, A1AT, and

Table 1. Subject Anthropometric and Clinical Values (Mean and Standard Deviation) before and after FF and Med Diet

	FF		Med	
variable	pre mean (SD)	post mean (SD)	pre mean (SD)	post mean (SD)
height (m)	1.71 (0.09)	1.71 (0.09)	1.71 (0.09)	1.71 (0.09)
weight (kg)	68.90 (12.92)	69.23 (13.18)	69.24 (13.08)	68.51 (12.91)
BMI (kg/m^2)	24.33 (3.69)	24.46 (3.88)	24.47 (3.79)	24.21 (3.67)
age (years)	22.10 (2.33)	22.10 (2.33)	22.10 (2.33)	22.10 (2.33)
systolic blood pressure	122.93 (14.53)	123.57 (17.83)	118.93 (9.75)	121.10 (12.58)
diastolic blood pressure	77.63 (14.30)	76.63 (13.25)	76.37 (7.27)	75.63 (8.43)
waist circumference (cm)	76.63 (9.83)	76.63 (9.83)	76.63 (9.83)	76.63 (9.83)
hip circumference (cm)	99.88 (6.97)	99.88 (6.97)	99.88 (6.97)	99.88 (6.97)
total cholesterol (mg/dL)	151.00 (30.92)	154.00 (18.10)	162.20 (16.04)	148.90 (17.93)
HDL-cholesterol (mg/dL)	51.10 (14.37)	53.89 (13.14)	52.80 (12.43)	50.50 (10.82)
LDL cholesterol (mg/dL)	87.10 (22.34)	87.67 (11.39)	93.00 (16.13)	86.50 (15.15)
triglycerides (mg/dL)	64.40 (24.22)	61.78 (21.78)	82.70 (29.72)	59.60 (20.05)

A2HSG were mentioned in the previously published report, and the transitions for ApoE are listed in Supplementary Table S2. The dMRM data were analyzed using Agilent Mass Hunter quantitative analysis software version B-05−02/build 5.2.365.0.

The glycoforms were named in the format of protein, position, N/O glycan, and glycan composition. The glycan composition is a four-digit number where each digit represents the number of hexose (Hex) (mannose or galactose), *N*-acetylhexosamine (HexNAc) (*N*-acetylgalactosamine), fucose (Fuc), and *N*-acetylneuraminic acid or sialic acid (Neu5Ac). For example, ApoE_290_O_1101 represents the glycopeptide of ApoE with an O-linked glycan consisting of 1 Hex, 1 HexNAc, 0 Fuc, and 1 Neu5Ac attached at position 290. The intensities of all glycoforms were normalized to the unglycosylated indicator peptide of the corresponding protein.

HDL ApoA-I and Cholesterol Efflux Assay

HDL ApoA-I was measured using the human apolipoprotein AI ELISA kit (ab189576) from Abcam (Cambridge, MA) in isolated HDL fractions. HDL cellular cholesterol efflux ability was measured via a commercially available kit (Abcam, ab196985) according to the manufacturer's instructions with the following modifications. Peripheral blood mononuclear cells (PBMCs) were isolated from healthy blood donors via Ficoll gradient extraction. Isolated PBMCs were then cultured in RPMI 1640 without HEPES containing 1× PSG and 10% FBS and T- and B-cell populations removed via adhesion properties. Remaining adherent PBMCs were differentiated into macrophage with 20 ng/mL of human macrophage colony-stimulating factor for 72 h. Fully differentiated macrophage cells were then lipid loaded using fluorescently labeled cholesterol (BODIPY) for 4 h, washed, and incubated with isolated HDL samples and assay controls for an additional 4 h. The volume of each HDL sample added was calculated to deliver 25 μg total protein based on the protein concentration of the isolated HDL fraction measured by nanodrop. The final volume in each well was constant. ACAT inhibitor and cAMP, which induces cholesterol efflux by the ATP binding cassette A1 (ABCA1), are included in the kit reagent. Cellular supernatant was removed and transferred to a new plate and cells were lysed using M-PER cell lysis buffer. Concentrations of fluorescently labeled cholesterol present in the supernatant and the cells were then measured separately using a microplate reader (Synergy H1 Hybrid Multi-Mode Reader, BioTek, VT), with the emission and excitation wavelengths of 482 and 515 nm, respectively. The percentage cholesterol efflux is calculated as below

$$\% \text{ chol efflux} = \frac{\text{fluorescence intensity of media}}{\text{fluorecence intensity of cell lysate + media}} \times 100\%$$

HDL Immunomodulatory Assay

Isolated HDL from each subject was supplemented into the media (RPMI 1640, 10% FBS, 1× PSG) of primary PBMCs (4 × 10^4 cells/well) at a normalized concentration of 1 mg/mL of protein for 1 h before exposing the HDL-cell mixture to 20 μg/mL of citrullinated fibrinogen immune complexes (cFb-IC) as an inflammatory stimulant specific to the Fc-γ receptor pathway.[32] Cells were incubated for 18 h to allow time for cytokine secretion after which the supernatants of each reaction were collected and TNF-α was measured by ELISA (Peprotech, Rocky Hill, NJ). Additionally, a positive control reaction consisting of PBMCs stimulated with cFb-ICs without any added HDL and a negative control consisting of unstimulated PBMCs were used to assess the effects of HDL on PBMC cytokine secretion. The % TNF-α suppression was calculated as below

$$\% \text{ TNF-}\alpha \text{ suppression}$$
$$= \left(1 - \frac{\text{TNF-}\alpha \text{ (ng/mL) in sample}}{\text{TNF-}\alpha \text{ (ng/mL) in positive control}}\right) \times 100\%$$

Statistical Analysis

The total amount of each protein (ApoE, ApoC-III, A1AT, A2HSG, and SAA) was quantified as the total intensity for the unglycosylated peptide with the highest response (i.e., indicator peptide) divided by the total protein amount in the isolated HDL fraction measured by nanodrop. For the glycoform quantification, the intensity of each glycopeptide was normalized to the intensity of its corresponding unglycosylated indicator peptide.

A differential abundance test was applied to the normalized site-specific glycosylation data using a mixed linear model, with the R package, limma.[33] Multiple test correction was performed on the *p*-values using the Benjamini−Hochberg method whenever more than 10 variables were tested. The same linear model was also applied on HDL cholesterol efflux, TNF-α suppression, and HDL ApoA-I level. Data were log2 transformed before linear model analysis and the shapiro.test function in R was used to perform the Shapiro−Wilk test of
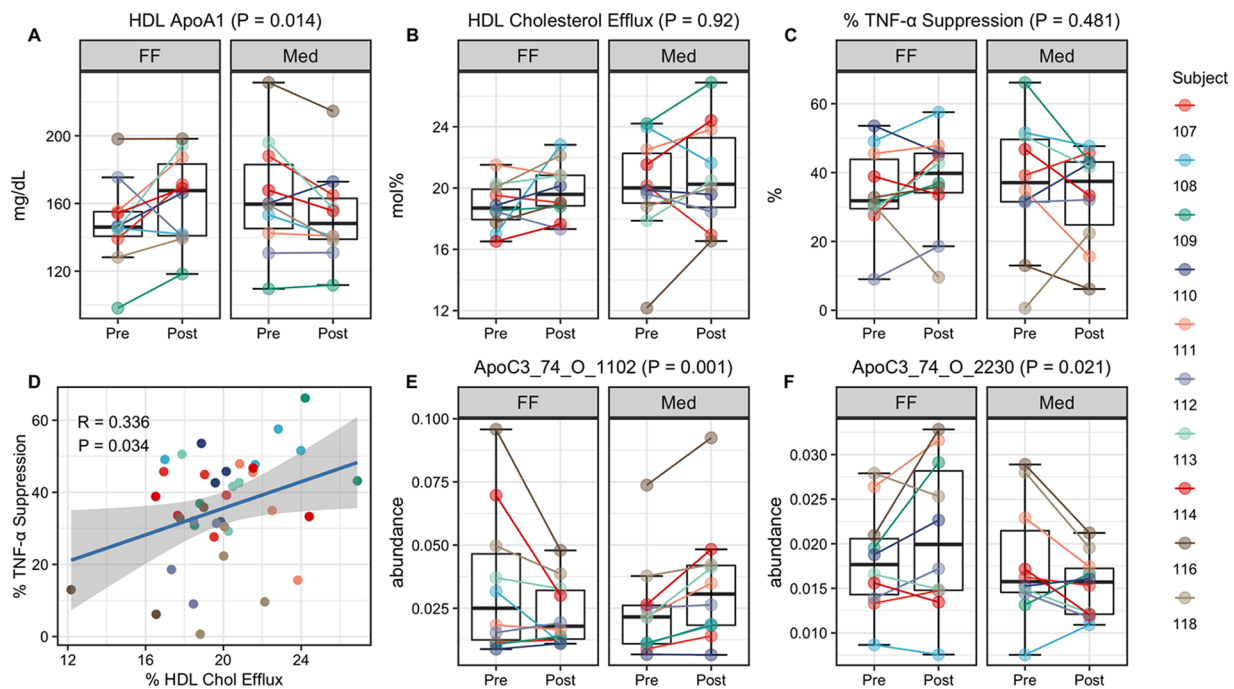
Figure 1. (A−C) Box plots of HDL ApoAI (mg/dL) (A), % HDL cholesterol efflux (B), and % macrophage TNF-α suppression (C) for subjects before and after FF and Med diets, with unadjusted P values. Lines with the same color represent the same subjects. (D) Scatter plot of % HDL cholesterol efflux and % TNF-α suppression. (E, F) Box plots of HDL glycans ApoC3_74_O_1102 and ApoC3_74_O_2230 before and after FF and Med diets, with unadjusted P values.
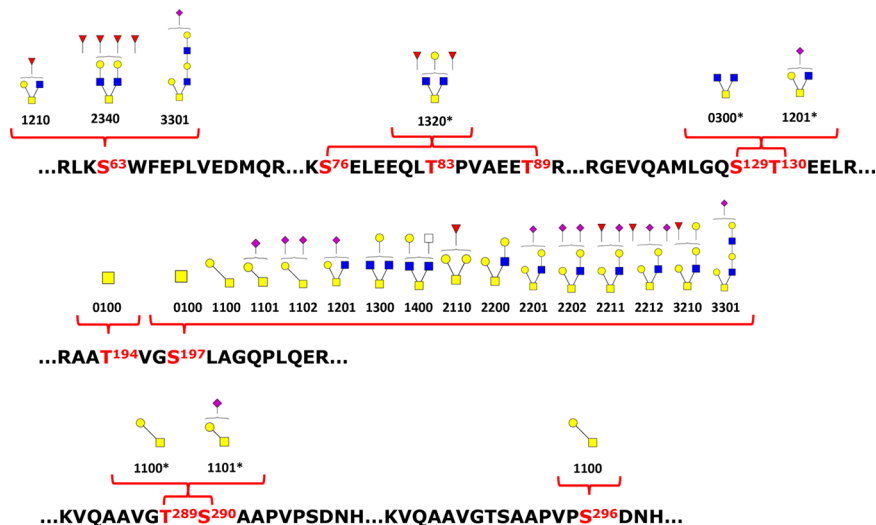

Figure 2. Glycan site heterogeneity of HDL-associated ApoE. Sites of attachment identified include Ser[63], Ser[76]/Thr[83]/Thr[89], Ser[129]/Thr[130], Thr[194], Ser[197], Thr[289]/Ser[290], and Ser[296]. The 4-digit glycan composition number corresponds to the number of hexose (Hex), N-acetylhexosamine (HexNAc) (which could be either N-acetylglucosamine (GlcNAc) or N-acetyl-galactosamine (GalNAc)), fucose (Fuc), and N-acetylneuraminic acid (NeuSAc) or sialic acid. A glycan containing 1 Hex, 1 HexNAc, 0 Fuc, and 2 NeuSAc is designated as 1102. Yellow square: GalNAc; blue square: GlcNAc; yellow circle: Gal; red triangle: Fuc; purple diamond: NeuSAc. *: multiple possible O-glycosylation sites for this glycan.

normality. The Pearson's correlation test was applied to find the correlation between different variables.

RESULTS

Baseline Characteristics and Dietary Records

All anthropometric values, blood pressure, and blood lipid levels were in the expected ranges and did not change significantly across the study period (Table 1). The BMIs showed that subjects were normal to slightly overweight. Summary data from the 3-day diet records from baseline and during the two study treatments are listed in Supplementary Table S3. The total calorie intake of each subject was relatively equivalent to their baseline level. The daily calorie intake at baseline was not statistically significantly different from FF (p = 0.506) or Med (p = 0.277). Carbohydrate intake was not significantly different between the two treatments.

HDL ApoA-I Content and Functional Measures

The average HDL ApoA-I concentration measured in this study population was 156.96 ($\pm$28.81) mg/dL. The change in HDL ApoA-I was statistically significant by mixed linear model
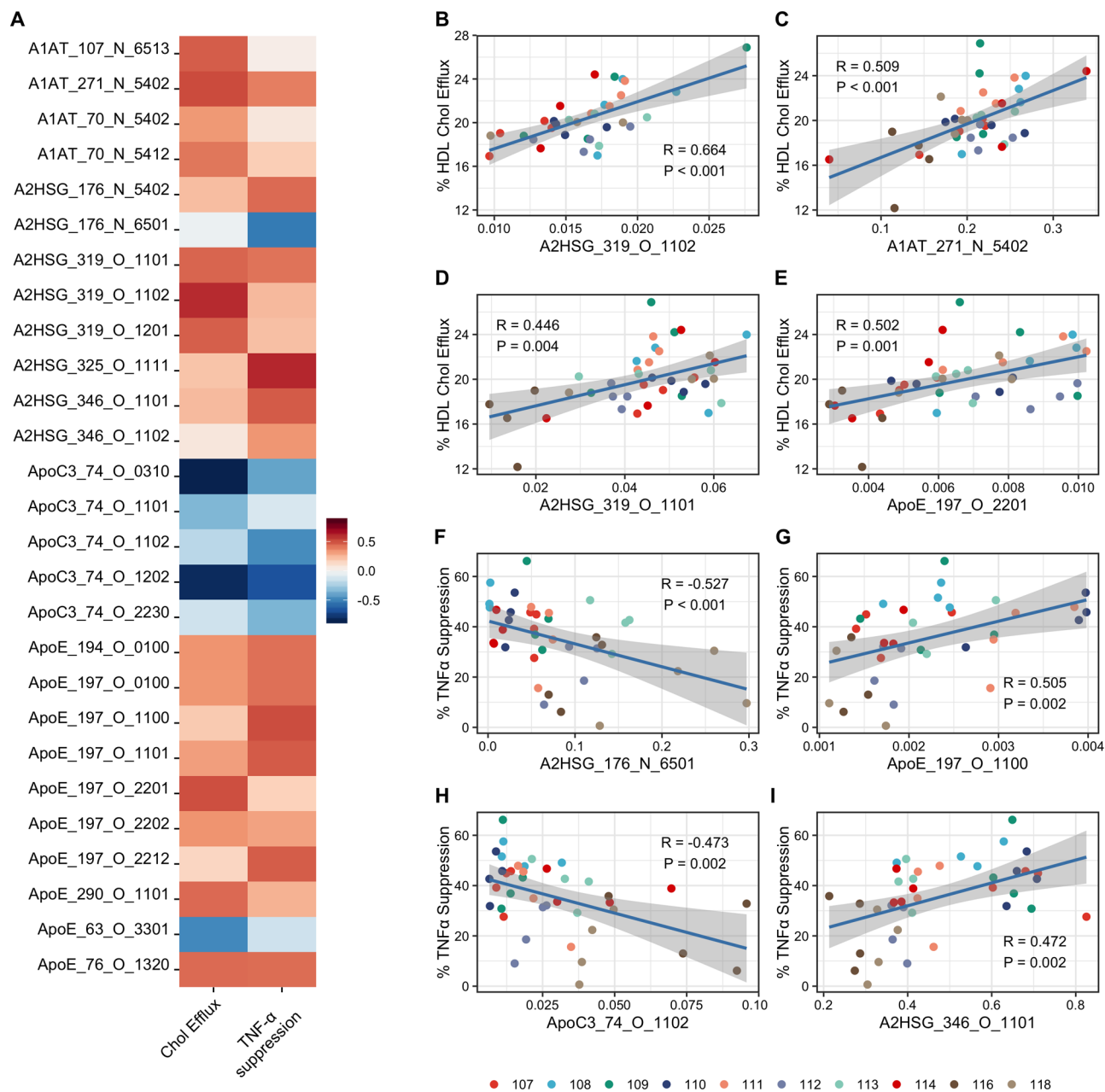
Figure 3. (A) Heatmap of Spearman's rho values between glycoforms and HDL functions. Glycans with $p < 0.05$ were selected. (B−E) Scatter plot of glycoforms A2HSG_319_O_1102 (B), A1AT_271_N_5402 (C), A2HSG_319_O_1101 (D), and ApoE_197_O_2201 (E) correlated with HDL cholesterol efflux capacity. (F−I) Scatter plot of glycoforms A2HSG_176_N_6501 (F), ApoE_197_O_1100 (G), ApoC3_74_O_1102 (H), and A2HSG_346_O_1101 (I) correlated with % TNF-α suppression.

analysis ($p = 0.015$ (Figure 1A)). The increase after FF was not statistically significant, but the decrease after Med was statistically significant ($p = 0.043$). Neither the cholesterol efflux capacity (18.85 ± 1.54 and $19.85 \pm 1.82\%$ before and after FF, and 20.07 ± 3.50 and $20.88 \pm 3.34\%$ before and after Med) nor the capacity to suppress TNF-α by stimulated macrophages (0.35 ± 0.13 and $0.37 \pm 0.14\%$ before and after FF, and 0.37 ± 0.19 and $0.33 \pm 0.14\%$ before and after Med) were significantly affected by either of the dietary interventions (Figure 1B,C). HDL cholesterol efflux capacity was positively associated with TNF-α suppression (rho = 0.304, $p = 0.057$; Figure 1D).

HDL Glycopeptides

Eighty-six glycopeptides were detected across the 4 measured proteins across all samples. ApoE was added to the existing

MRM site-specific glycosylation method described previously.[10] Four glycosylation sites (Thr[194], Ser[197], Ser[263], and Ser[296]) and three putative glycosylation sites (Ser[129]/Thr[130]Ser[76]/Thr[83]/Thr[89], and Thr[289]/Ser[290]) were detected. The three putative glycosylation sites have multiple possible O-glycan linkage sites (serine and threonine) in the fragmented peptides; thus, it is not possible to determine to which exact amino acid the glycans are attached. Across these 7 glycosylation sites, a total of 25 glycoforms were detected and monitored. The sites and structures are shown in Figure 2. The glycans found on ApoE include a simple attachment of a GalNAc residue (e.g., 0100 on site 194), nonsialylated, nonfucosylated structures (e.g., 2200 on site 197) monosialylated structures (e.g., 1201 on site 129), disialylated structures (e.g., 1102 on site 197), and previously

unidentified fucosylated structures (e.g., 2110 on site 197). ApoE glycopeptides were not affected by dietary treatment.

The two most abundant ApoC-III glycans, ApoC3_74_O_1102 and ApoC3_74_O_2230, were differentially affected by diet. The disialylated glycopeptide ApoC3_74_O_1102 decreased after FF and increased after Med, whereas the nonsialylated glycopeptide ApoC3_74_O_2230 increased after FF and decreased after Med (unadjusted p = 0.001 and 0.021, respectively; Figure 1E,F). However, they did not remain statistically significant after adjustment for multiple testing (adjusted p = 0.089, adjusted). Supplementary Table S4 lists all glycopeptides with their relative abundance before and after FF and Med, as well as their linear mixed model p values. The abundance of the indicator peptides (i.e., the quantity) of all measured proteins were also not differentially affected by dietary treatment (Supplementary Table S5).

Although most HDL glycopeptides were not affected differently by diet, many of them were correlated with HDL function. Supplementary Figures S1 and S2 are histograms of Pearson's p values between each glycopeptide and HDL cholesterol efflux and TNF-α suppression capacity. Out of the 86 measured HDL glycoforms, 25 were significantly correlated with HDL cholesterol eflux and 21 with TNF-α suppression. Figure 3A shows the 27 features that were correlated with either HDL cholesterol efflux capacity or TNF-α suppression with the Spearman's test. The Spearman's test was used here to reduce the effect of outliers. Glycosylations on A1AT, A2HSG, and ApoE were generally positively correlated with HDL cholesterol efflux capacity and macrophage TNF-α suppression, while ApoC-III glycans were negatively correlated with HDL cholesterol efflux and TNF-α suppression. Figure 3B-I shows 8 site-specific glycans significantly correlated with HDL cholesterol efflux or TNF-α suppression after multiple test adjustments ($p < 0.05$, adjusted).

■ DISCUSSION

There is agreement that improving HDL functional capacity is a desirable strategy for preventing disease and improving the outcomes associated with dyslipidemia. However, it is not at all clear how to improve HDL functional capacity. Since diet can modify HDL functional capacity by altering its composition and, at the same time, is a major potential source of background variance in free-living individuals, we set out to define the impact of diet on HDL composition and function at the time scale of 4 days. We were interested in the effects of diet on the quantities and glycoprofiles of key HDL-associated proteins, and whether HDL glycoprofiles are associated with HDL functional capacity. In particular, ApoE is of great interest due to known associations with Alzheimer's and cardiovascular disease risks.[34,35] ApoE structure is also known to affect lipoprotein metabolism.[36,37] It is not yet clear how glycosylation of ApoE affects its structure and function in the context of HDL particles, although it has already been shown that ApoE desialylation reduces binding to HDL and increases binding to VLDL.[38]

ApoE does not contain the consensus amino acid sequence (NX(T/S/C)) for N-linked glycosylation and instead is O-glycosylated with mucin-type glycans at Thr[194], which is not essential for ApoE secretion.[39] It was also confirmed by a recent study that Thr[212] is a glycosylation site.[40] ApoE secreted by macrophages isolated from PBMCs of a single donor with the ApoE3/E3 genotype had 8 different non-, mono-, and disialylated glycoforms at site Thr[194] and 3 putative new sites

were identified at Ser[290], Thr[289], and Ser[296].[41] In this study, we report for the first time 4 additional O-glycosylation sites in HDL-associated ApoE, with glycans attached ranging from simple GlcNAc to biantennary structures containing both sialic acid and fucose. Future studies are needed to determine the exact sites of glycan attachment in the three putative glycosylation sites found in this study.

The glycoprofile of ApoE was not affected by short-term diet in this study. The glycans attached to A1AT and A2HSG were also not changed in response to diet at the time scale tested in this study. Two ApoC-III sialylated glycans were changed by diet but did not remain statistically significant after adjustment for multiple testing. In our previous study, the glycan ApoC3_74_O_1102, which decreased after FF and increased after Med in this study, was found to be 2-fold higher in HDL compared to that in plasma[10] and elevated in hemodialysis patients but decreased in MetS patients compared to that in healthy human controls.[12] Although the glycan ApoC3_74_O_2230, which increased after FF and decreased after Med in this study, was not detected in our previous study, another nonsialylated ApoC-III glycan, ApoC3_74_O_0300, was found to be decreased in hemodialysis patients and elevated in MetS patients.[12] Disialylated ApoC-III was enriched in small dense LDL in hemodialysis patients with dyslipidemia[42] and was found to be reduced across lipoprotein classes in MetS patients.[43] This suggests that the sialylation of HDL-associated ApoC-III is altered by underlying physiological or disease state as well as by short-term dietary changes.

It has been shown previously that HDL ApoA-I content is associated with cholesterol efflux capacity.[44] However, although HDL ApoA-I content decreased on the Med diet and increased on the FF diet, neither of the two HDL functional capacities tested were significantly altered in response to the diets. It is not clear whether the lack of effect of diet on HDL cholesterol efflux capacity, capacity to suppress TNF-α secretion in cFb-IC-stimulated monocytes, and HDL-associated ApoE, A1AT, and A2HSG content and glycoprofiles are due to the study duration or the sample size, or whether there is truly no effect of dietary changes of the type tested in this study on these HDL compositional and functional measures. Future studies are needed to determine the longer-term effects of diet, the effects of individual dietary components, and the effects of diet in larger cohorts of individuals.

Despite the lack of effect of short-term diet change, the results from this study suggest that the glycoprofiles of HDL-associated proteins are highly correlated with both cholesterol efflux and immunomodulatory capacity. The functional role of glycosylation of HDL proteins is not yet known. Multiple glycopeptides on A1AT, A2HSG, and ApoE were positively correlated, whereas ApoC-III glycopeptides were generally negatively correlated with both HDL functional measures. In a previous study we found that HDL that suppressed IL-6 production in LPS-stimulated monocytes were enriched in disialylated A2HSG, particularly A2HSG_176_N_5402;[12] in this study, we similarly found a positive correlation between A2HSG_176_N_5402 and both HDL functional measures. We previously found that both 5402 and 5412 attached at multiple sites of A1AT were decreased in HDL, which suppressed IL-6 production in LPS-stimulated monocytes;[12] however, in this study, we found that glycopeptides containing these disialylated glycans were positively correlated with cholesterol efflux capacity and the capacity to suppress TNF-α secretion in cFb-IC-stimulated monocytes. More studies are

needed to understand how glycosylation affects the structural and functional characteristics of HDL particles and how glycans alter the cell—surface interactions between HDL particles and different cell types expressing different cell surface HDL receptors.

CONCLUSIONS

In this study, we report for the first time that ApoE has 4 additional O-glycosylation sites that were not reported previously and describe an MRM method for profiling ApoE glycosylation. Whereas consuming two very different diets for 4 days did not affect the glycoprofile of ApoE, A1AT, or A2HSG associated with HDL particles, the quantities of these proteins, or the two HDL functional capacities we measured, HDL-associated ApoC-III sialylation, and quantity of ApoA-I were altered. Our results suggest that the overall HDL glycoproteomic composition may be more highly influenced by factors other than diet in the short term and thus may be more indicative of longer-term processes and/or disease conditions; however, ApoC-III sialylation may be more directly responsive to short-term dietary change. Our results also revealed that HDL functionality is strongly associated with HDL glycoproteomic composition, and the mechanisms and implications of this association need to be further studied in future studies.

ASSOCIATED CONTENT

ⓈSupporting Information

The Supporting Information is available free of charge on the ACS Publications website at DOI: 10.1021/acs.jproteome.9b00450.

> Study diet menu on the FF arm (2000 kcal/day) (Supplementary Table S1); ApoE glycopeptides, precursor, product, retention time, collision energy, and peptide bearing the glycan (Supplementary Table S2); Macronutrient composition of diet at baseline and after dietary treatment (Supplementary Table S3); relative abundance of glycopeptides before and after treatments, and their statistical p values (Supplementary Table S4); relative abundance of HDL proteins before and after treatments, and their statistical p values, measured by mass spectrometry (Supplementary Table S5); histogram of Pearson's p values between HDL glycoforms and HDL cholesterol efflux capacity (Supplementary Figure S1); histogram of Pearson's p values between HDL glycoforms and HDL % TNF-α suppression of macrophage cells (Supplementary Figure S2) (PDF)

AUTHOR INFORMATION

Corresponding Author

*E-mail: amzivkovic@ucdavis.edu.

ORCID Ⓞ

Chenghao Zhu: 0000-0003-1674-4533
Qiongyu Li: 0000-0003-3654-0378
Carlito B. Lebrilla: 0000-0001-7190-5323
Angela M. Zivkovic: 0000-0002-2828-7862

Notes

The authors declare no competing financial interest.

ABBREVIATIONS

ApoE, apolipoprotein E; ApoC-III, apolipoprotein C-III; A1AT, α-1-antitrypsin; A2HSG, α-2-HS-glycoprotein; CVD, cardiovascular disease; T2D, type 2 diabetes; FF, fast food; Med, Mediterranean

REFERENCES

(1) Ansell, B. J.; Fonarow, G. C.; Fogelman, A. M. The Paradox of Dysfunctional High-Density Lipoprotein. *Curr. Opin. Lipidol.* **2007**, *18*, 427−434.

(2) Badimon, L.; Vilahur, G. LDL-Cholesterol Versus Hdl-Cholesterol in the Atherosclerotic Plaque: Inflammatory Resolution Versus Thrombotic Chaos. *Ann. N. Y. Acad. Sci.* **2012**, *1254*, 18−32.

(3) Soran, H.; Hama, S.; Yadav, R.; Durrington, P. N. HDL Functionality. *Curr. Opin. Lipidol.* **2012**, *23*, 353−366.

(4) Asztalos, B. F.; Tani, M.; Schaefer, E. J. Metabolic and Functional Relevance of Hdl Subspecies. *Curr. Opin. Lipidol.* **2011**, *22*, 176−185.

(5) Furtado, J. D.; Yamamoto, R.; Melchior, J. T.; Andraski, A. B.; Gamez-Guerrero, M.; Mulcahy, P.; He, Z.; Cai, T.; Davidson, W. S.; Sacks, F. M. Distinct Proteomic Signatures in 16 Hdl (High-Density Lipoprotein) Subspecies. *Arterioscler., Thromb., Vasc. Biol.* **2018**, *38*, 2827−2842.

(6) Vaisar, T.; Tang, C.; Babenko, I.; Hutchins, P.; Wimberger, J.; Suffredini, A. F.; Heinecke, J. W. Inflammatory remodeling of the HDL proteome impairs cholesterol efflux capacity. *J. Lipid Res.* **2015**, *56*, 1519−1530.

(7) Alwaili, K.; Bailey, D.; Awan, Z.; Bailey, S. D.; Ruel, I.; Hafiane, A.; Krimbou, L.; Laboissiere, S.; Genest, J. The Hdl Proteome in Acute Coronary Syndromes Shifts to an Inflammatory Profile. *Biochim. Biophys. Acta, Mol. Cell Biol. Lipids* **2012**, *1821*, 405−415.

(8) Heinecke, J. W. The Hdl Proteome: A Marker−and Perhaps Mediator−of Coronary Artery Disease. *J. Lipid Res.* **2009**, *50*, S167−S171.

(9) Huang, J.; Lee, H.; Zivkovic, A. M.; Smilowitz, J. T.; Rivera, N.; German, J. B.; Lebrilla, C. B. Glycomic Analysis of High Density Lipoprotein Shows a Highly Sialylated Particle. *J. Proteome Res.* **2014**, *13*, 681−691.

(10) Kailemia, M. J.; Wei, W.; Nguyen, K.; Beals, E.; Sawrey-Kubicek, L.; Rhodes, C.; Zhu, C.; Sacchi, R.; Zivkovic, A. M.; Lebrilla, C. B. Targeted Measurements of O- and N-Glycopeptides Show That Proteins in High Density Lipoprotein Particles Are Enriched with Specific Glycosylation Compared to Plasma. *J. Proteome Res.* **2018**, *17*, 834−845.

(11) Krishnan, S.; Huang, J.; Lee, H.; Guerrero, A.; Berglund, L.; Anuurad, E.; Lebrilla, C. B.; Zivkovic, A. M. Combined High-Density Lipoprotein Proteomic and Glycomic Profiles in Patients at Risk for Coronary Artery Disease. *J. Proteome Res.* **2015**, *14*, 5109−5118.

(12) Krishnan, S.; Shimoda, M.; Sacchi, R.; Kailemia, M. J.; Luxardi, G.; Kaysen, G. A.; Parikh, A. N.; Ngassam, V. N.; Johansen, K.; Chertow, G. M.; et al. HDL Glycoprotein Composition and Site-Specific Glycosylation Differentiates Between Clinical Groups and Affects Il-6 Secretion in Lipopolysaccharide-Stimulated Monocytes. *Sci. Rep.* **2017**, *7*, No. 43728.

(13) Egert, S.; Rimbach, G.; Huebbe, P. ApoE Genotype: From Geographic Distribution to Function and Responsiveness to Dietary Factors. *Proc. Nutr. Soc.* **2012**, *71*, 410−424.

(14) Corder, E. H.; Saunders, A. M.; Strittmatter, W. J.; Schmechel, D. E.; Gaskell, P. C.; Small, G. W.; Roses, A. D.; Haines, J. L.; Pericak-Vance, M. A. Gene Dose of Apolipoprotein E Type 4 Allele and the Risk of Alzheimer's Disease in Late Onset Families. *Science* **1993**, *261*, 921–923.

(15) Matsuura, F.; Wang, N.; Chen, W.; Jiang, X.-C.; Tall, A. R. HDL from Cetp-Deficient Subjects Shows Enhanced Ability to Promote Cholesterol Efflux from Macrophages in an apoE- and Abcg1-Dependent Pathway. *J. Clin. Invest.* **2006**, *116*, 1435–1442.

(16) Pamir, N.; Hutchins, P.; Ronsein, G.; Vaisar, T.; Reardon, C. A.; Getz, G. S.; Lusis, A. J.; Heinecke, J. W. Proteomic Analysis of Hdl from Inbred Mouse Strains Implicates Apoe Associated with Hdl in Reduced Cholesterol Efflux Capacity via the Abca1 Pathway. *J. Lipid Res.* **2016**, *57*, 246–257.

(17) Andersen, C. J.; Blesso, C. N.; Lee, J.; Barona, J.; Shah, D.; Thomas, M. J.; Fernandez, M. L. Egg Consumption Modulates Hdl Lipid Composition and Increases the Cholesterol-Accepting Capacity of Serum in Metabolic Syndrome. *Lipids* **2013**, *48*, 557–567.

(18) Andersen, C. J.; Fernandez, M. L. Dietary Approaches to Improving Atheroprotective Hdl Functions. *Food Funct.* **2013**, *4*, 1304–1313.

(19) Thompson, P. D.; Cullinane, E. M.; Sady, S. P.; Flynn, M. M.; Bernier, D. N.; Kantor, M. A.; Saritelli, A. L.; Herbert, P. N. Modest Changes in High-Density Lipoprotein Concentration and Metabolism with Prolonged Exercise Training. *Circulation* **1988**, *78*, 25–34.

(20) Zhu, C.; Sawrey-Kubicek, L.; Beals, E.; Hughes, R. L.; Rhodes, C. H.; Sacchi, R.; Zivkovic, A. M. The Hdl Lipidome Is Widely Remodeled by Fast Food Versus Mediterranean Diet in 4 Days. *Metabolomics* **2019**, *15*, 114.

(21) Bahadoran, Z.; Mirmiran, P.; Golzarand, M.; Hosseini-Esfahani, F.; Azizi, F. Fast Food Consumption in Iranian Adults; Dietary Intake and Cardiovascular Risk Factors: Tehran Lipid and Glucose Study. *Arch. Iran. Med.* **2012**, *15*, 346–351.

(22) Deng, F. E.; Shivappa, N.; Tang, Y.; Mann, J. R.; Hebert, J. R. Association Between Diet-Related Inflammation, All-Cause, All-Cancer, and Cardiovascular Disease Mortality, with Special Focus on Prediabetics: Findings from NHANES III. *Eur. J. Nutr.* **2017**, *56*, 1085–1093.

(23) Garcia-Arellano, A.; Ramallal, R.; Ruiz-Canela, M.; Salas-Salvadó, J.; Corella, D.; Shivappa, N.; Schröder, H.; Hébert, J. R.; Ros, E.; Gómez-Garcia, E.; et al. Dietary Inflammatory Index and Incidence of Cardiovascular Disease in the Predimed Study. *Nutrients* **2015**, *7*, 4124–4138.

(24) O'Neil, A.; Shivappa, N.; Jacka, F. N.; Kotowicz, M. A.; Kibbey, K.; Hebert, J. R.; Pasco, J. A. Pro-Inflammatory Dietary Intake as a Risk Factor for Cvd in Men: A 5-Year Longitudinal Study. *Br. J. Nutr.* **2015**, *114*, 2074–2082.

(25) Nettleton, J. A.; Steffen, L. M.; Mayer-Davis, E. J.; Jenny, N. S.; Jiang, R.; Herrington, D. M.; Jacobs, D. R., Jr. Dietary Patterns Are Associated with Biochemical Markers of Inflammation and Endothelial Activation in the Multi-Ethnic Study of Atherosclerosis (MESA). *Am. J. Clin. Nutr.* **2006**, *83*, 1369–1379.

(26) Estruch, R. Anti-Inflammatory Effects of the Mediterranean Diet: The Experience of the Predimed Study. *Proc. Nutr. Soc.* **2010**, *69*, 333–340.

(27) Estruch, R.; Ros, E.; Salas-Salvadó, J.; Covas, M.-I.; Corella, D.; Arós, F.; Gómez-Gracia, E.; Ruiz-Gutiérrez, V.; Fiol, M.; Lapetra, J.; et al. Primary Prevention of Cardiovascular Disease with a Mediterranean Diet. *N. Engl. J. Med.* **2013**, *368*, 1279–1290.

(28) Martínez-Lapiscina, E. H.; Clavero, P.; Toledo, E.; Estruch, R.; Salas-Salvadó, J.; San Julián, B.; Sanchez-Tainta, A.; Ros, E.; Valls-Pedret, C.; Martinez-Gonzalez, M. Á. Mediterranean Diet Improves Cognition: The Predimed-Navarra Randomised Trial. *J. Neurol., Neurosurg. Psychiatry* **2013**, *84*, 1318–1325.

(29) Salas-Salvadó, J.; Bulló, M.; Babio, N.; Martínez-González, M. Á.; Ibarrola-Jurado, N.; Basora, J.; Estruch, R.; Covas, M. I.; Corella, D.; Arós, F.; et al. Reduction in the Incidence of Type 2 Diabetes with the Mediterranean Diet: Results of the Predimed-Reus Nutrition Intervention Randomized Trial. *Diabetes Care* **2011**, *34*, 14–19.

(30) Salas-Salvadó, J.; Fernández-Ballart, J.; Ros, E.; Martínez-González, M.-A.; Fitó, M.; Estruch, R.; Corella, D.; Fiol, M.; Gómez-Gracia, E.; Arós, F.; et al. Effect of a Mediterranean Diet Supplemented with Nuts on Metabolic Syndrome Status: One-Year Results of the Predimed Randomized Trial. *Arch. Intern. Med.* **2008**, *168*, 2449–2458.

(31) Serra-Majem, L.; Roman, B.; Estruch, R. Scientific Evidence of Interventions Using the Mediterranean Diet: A Systematic Review. *Nutr. Rev.* **2006**, *64*, S27–S47.

(32) Sokolove, J.; Zhao, X.; Chandra, P. E.; Robinson, W. H. Immune Complexes Containing Citrullinated Fibrinogen Costimulate Macrophages via Toll-Like Receptor 4 and Fcγ Receptor. *Arthritis Rheum.* **2011**, *63*, 53–62.

(33) Ritchie, M. E.; Phipson, B.; Wu, D.; Hu, Y.; Law, C. W.; Shi, W.; Smyth, G. K. Limma Powers Differential Expression Analyses for Rna-Sequencing and Microarray Studies. *Nucleic Acids Res.* **2015**, *43*, No. e47.

(34) Mahoney-Sanchez, L.; Belaidi, A. A.; Bush, A. I.; Ayton, S. The Complex Role of Apolipoprotein E in Alzheimer's Disease: An Overview and Update. *J. Mol. Neurosci.* **2016**, *60*, 325–335.

(35) Deane, R.; Sagare, A.; Hamm, K.; Parisi, M.; Lane, S.; Finn, M. B.; Holtzman, D. M.; Zlokovic, B. V. ApoE Isoform-Specific Disruption of Amyloid Beta Peptide Clearance from Mouse Brain. *J. Clin. Invest.* **2008**, *118*, 4002–4013.

(36) Okoro, E. U.; Zhao, Y.; Guo, Z.; Zhou, L.; Lin, X.; Yang, H. Apolipoprotein E4 Is Deficient in Inducing Macrophage Abca1 Expression and Stimulating the Sp1 Signaling Pathway. *PLoS One* **2012**, *7*, No. e44430.

(37) Heeren, J.; Grewal, T.; Laatsch, A.; Becker, N.; Rinninger, F.; Rye, K.-A.; Beisiegel, U. Impaired Recycling of Apolipoprotein E4 Is Associated with Intracellular Cholesterol Accumulation. *J. Biol. Chem.* **2004**, *279*, 55483–55492.

(38) Ghosh, P.; Hale, E. A.; Mayur, K.; Seddon, J.; Lakshman, M. R. Effects of Chronic Alcohol Treatment on the Synthesis, Sialylation, and Disposition of Nascent Apolipoprotein E by Peritoneal Macrophages of Rats. *Am. J. Clin. Nutr.* **2000**, *72*, 190–198.

(39) Wernette-Hammond, M. E.; Lauer, S. J.; Corsini, A.; Walker, D.; Taylor, J. M.; Rall, S. Glycosylation of Human Apolipoprotein E. The Carbohydrate Attachment Site Is Threonine 194. *J. Biol. Chem.* **1989**, *264*, 9094–9101.

(40) Mancone, C.; Amicone, L.; Fimia, G. M.; Bravo, E.; Piacentini, M.; Tripodi, M.; Alonzi, T. Proteomic Analysis of Human Very Low-Density Lipoprotein by Two-Dimensional Gel Electrophoresis and Maldi-Tof/Tof. *Proteomics* **2007**, *7*, 143–154.

(41) Lee, Y.; Kockx, M.; Raftery, M. J.; Jessup, W.; Griffith, R.; Kritharides, L. Glycosylation and sialylation of macrophage-derived human apolipoprotein E analyzed by SDS-PAGE and mass spectrometry: evidence for a novel site of glycosylation on Ser290. *Mol. Cell. Proteomics* **2010**, *9*, 1968–1981.

(42) Deighan, C. J.; Caslake, M. J.; McConnell, M.; Boulton-Jones, J. M.; Packard, C. J. Atherogenic Lipoprotein Phenotype in End-Stage Renal Failure: Origin and Extent of Small Dense Low-Density Lipoprotein Formation. *Am. J. Kidney Dis.* **2000**, *35*, 852–862.

(43) Savinova, O. V.; Fillaus, K.; Jing, L.; Harris, W. S.; Shearer, G. C. Reduced Apolipoprotein Glycosylation in Patients with the Metabolic Syndrome. *PLoS One* **2014**, *9*, No. e104833.

(44) Khera, A. V.; Cuchel, M.; de la Llera-Moya, M.; Rodrigues, A.; Burke, M. F.; Jafri, K.; French, B. C.; Phillips, J. A.; Mucksavage, M. L.; Wilensky, R. L.; et al. Cholesterol Efflux Capacity, High-Density Lipoprotein Function, and Atherosclerosis. *N. Engl. J. Med.* **2011**, *364*, 127–135.